2. ACCELERATOR AUGMENTATION PROGRAM

2.1 LINAC

S.Ghosh, A.Rai, P.Patra, G.K.Chowdhury, B.K.Sahu, A.Pandey, D.S.Mathuria, J.Karmakar, S.S.K.Sonti, K.K.Mistry, R.N.Dutt, A.Sarkar, R.Joshi, R. Ahuja, J.Chacko, A.Chowdhury, S.Kar, S.Babu, M.Kumar, J.Antony, J.Zacharias, P.N.Prakash, T.S.Datta, D.Kanjilal and A.Roy

2.1.1 OPERATION OF SUPERCONDUCTING LINAC & DELIVERY OF ENERGISED BEAM FOR NUCLEAR PHYSICS EXPERIMENTS

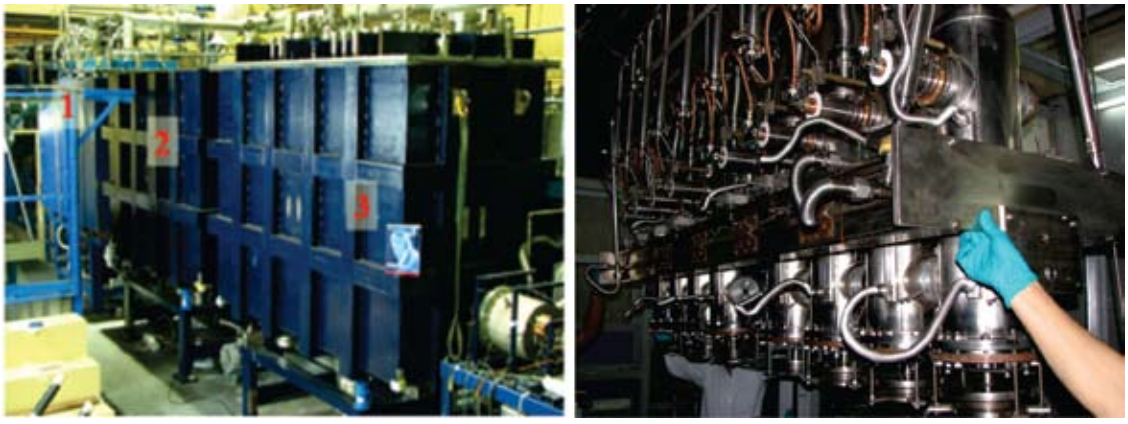

Fig. 1. The first picture shows the three accelerating module of the Superconducting Linear accelerator of IUAC. The second picture shows the second linac cryostats being installed in the beam line.

The complete linear accelerator (Linac) of Inter University Accelerator Centre consists of five cryostats, the first one acting as superbuncher consisting of a single quarter wave resonator (QWR), the next three linac cryomodules house eight QWRs each, and the last one has two QWRs used as rebuncher.

Table 1. The beam species and their total energies delivered for experiments

Beam	Pell. energy (MeV)	Linac energy gain (MeV)	Total energy (MeV)	Beam Line
$^{19}F^{+7}$	100	37	137	NAND
$^{28}Si^{+11}$	130	60	190	Linac Scattering chamber
		56	186	HYRA
$^{31}P^{+11}$	130	58	188	HYRA

In recent past, with the help of superbuncher, the first linac accelerating module and the rebuncher, Pelletron ion beams from ^{12}C to ^{107}Ag were further accelerated and delivered to conduct experiments in Nuclear Physics and Material Science. In 2011 another eight niobium resonators were installed in the linac cryostat-2 and a couple of off-line cold tests were conducted followed by beam acceleration through linac. During the beam acceleration, all sixteen resonators of cryostat 1 and 2 took part along with the single resonator operated each in superbuncher and rebuncher cryostat. During this entire period of beam acceleration extending for more than a month, three different beam species: ^{19}F, ^{28}Si and ^{31}P were accelerated and beam was delivered in the beam line of HYRA (Hybrid Recoil mass Analyzer) and NAND (National Array of Neutron Detectors). The results of the beam acceleration, in brief, are given in Table-1.

2.1.2 DEVELOPMENTAL ACTIVITIES IN LINAC

To increase the performance of the accelerating fields and hence the energy gain of the ion beam from the linac, several steps are adopted and they are listed in the following:

a) A warm water ultrasonic rinsing facility was installed for the final rinsing of the resonator before installation in the linac cryostat. It is observed that warm water ultrasonic rinsing reduces the field emission and helps to improve the accelerating fields of the niobium resonators.

b) A separate cooling arrangement for the power coupler of the resonator is designed and fabricated for the drive couplers of the resonators and that will be installed on the resonators of linac cryostat-3. This will protect the coupler and the power cable from overheating and help to increase the accelerating field of the resonators.

c) A separate tuning mechanism based on the Piezo actuator was designed and tested on a few resonators in the past. Now the same Piezo actuator based tuning mechanism is being implemented on a few resonators in linac cryostat-3. This new tuning mechanism will help to increase the accelerating fields of the resonators and to reduce the forward RF power required to phase lock a resonator.

d) The vibration damping mechanism of the resonators using SS-balls is re-investigated with the resonators built indigenously to explore the possibility of improvement of the damping efficiency. During this current investigation, SS-balls with bigger diameter (what was not tried before) and a mixture of SS-balls with different diameters are being tried out at room temperature and the results are encouraging. However, the whole experiment has to be validated at superconducting state of the resonators.

To make the Linac operation smoother and trouble free, an ambitious plan of automatic locking of the resonators (when they go out of phase lock occasionally) without any human intervention has been taken up and some substantial progress is also achieved. In the next beam acceleration, it is planned to incorporate this auto tuning mechanism on linac resonators.

Beam	Energy (Pell.) (MeV)	Total Energy (after linac-1 and 2) (MeV)	Predicted acceleration Phases of resonators in linac-1 and 2 to obtain minimum time width	Predicted reduction in delta_t (%)	Measured Time width (GPSC - II)	Actual reduction in delta_t (%)
$^{28}Si^{+11}$	130	186	All 70^0		2.88	
			70, 70, 110, 110, 110, 70, 70, 70 70, 70, 70, 70, 70, 70, 70, 110	62	1.73	66

Table 2. The calculated and measured values of the time width of $^{28}Si^{+11}$ at the user's target chamber

A simulation code was written to determine the optimum phase combination between 70 and 110 degrees for all the sixteen resonators in Linac cryostats 1 and 2 to obtain the minimum time width of the beam bunch delivered at the user's scattering chamber which is ~ 30 m far from the last (3rd) linac cryostat. During the previous linac operations, the accelerating phases for all the resonators were kept at 70 degree and the beam was delivered for experiments. The calculation shows that by changing the accelerating phases of a few resonators from 70 to 110 degrees will reduce the time width of the beam bunch substantially at the target location. The calculation was verified by experiments and an excellent match was observed between the theoretical prediction and experimental observation. This program is also useful to find out the optimum combination of all the accelerating resonators to reduce the load on the bunching mechanism of the rebuncher resonators. The reduction of the time width of the accelerated beam could be so drastic

that in some cases, we may not need to use the rebuncher at all when the time width requirement from the experimentalist is not very stringent (about ~ 1 nsec). The calculation and the experimental results from the data of linac acceleration are given in table 2.

At present, the installation work of the remaining eight resonators in the last accelerating module (number-3 in figure 1) of linac is going on. After that, a couple of offline cold tests are planned to validate the performances of the resonators installed in linac-3. After the successful off-line testing of linac, the operation of the complete linac and the delivery of the ion beam for scheduled experiments are expected to start by the middle of 2012.

2.1.3 SUPERCONDUCTING NIOBIUM RESONATORS

P.N.Prakash, K.K.Mistri, S.S.K.Sonti, A.Rai, J.Zacharias, S.Ghosh, P.Patra, G.K.Chowdhury, D.S.Mathuria, R.N.Dutt, A.Pandey, B.K.Sahu, D.Kanjilal & A.Roy

During the linac run the performance of several indigenously built quarter wave resonators (QWR) which could not be tested in the test cryostat, was found to be excellent. At 4.2 K the QWRs achieved very high accelerating gradients. The first prototype niobium low beta resonator has been completed. Bead pull measurements indicate very good agreement between the calculated and measured values of the parameters. Cold tests on the low beta resonator will be performed in the next weeks. Fabrication of the Single Spoke Resonators for Project-X at Fermi National Accelerator Laboratory (FNAL) has been slightly delayed due to the long breakdown of the electron beam welding machine. Two additional 1.3 GHz *improved single cell niobium cavities* were fabricated in collaboration with Raja Ramanna Centre for Advanced Technology (RRCAT), Indore and sent to Fermi Lab where they were tested at 2 K. Both the cavities have achieved gradients in excess of 35 MV/m, with one of them reaching 40 MV/m at 1.8 K. Fabrication of a 5-cell 1.3 GHz cavity has begun. There are plans to build 650 MHz β=0.6 and 0.9 single cell cavities also.

2.1.3.1 PERFORMANCE OF INDIGENOUSLY BUILT RESONATORS

The performance of the indigenously built QWRs has been excellent. In figure 1, CW gradients in linac / test cryostat for several resonators that were tested in either cryostat, is shown. The pulsed gradients (typical duty cycle ~25%) are 20-25% more.

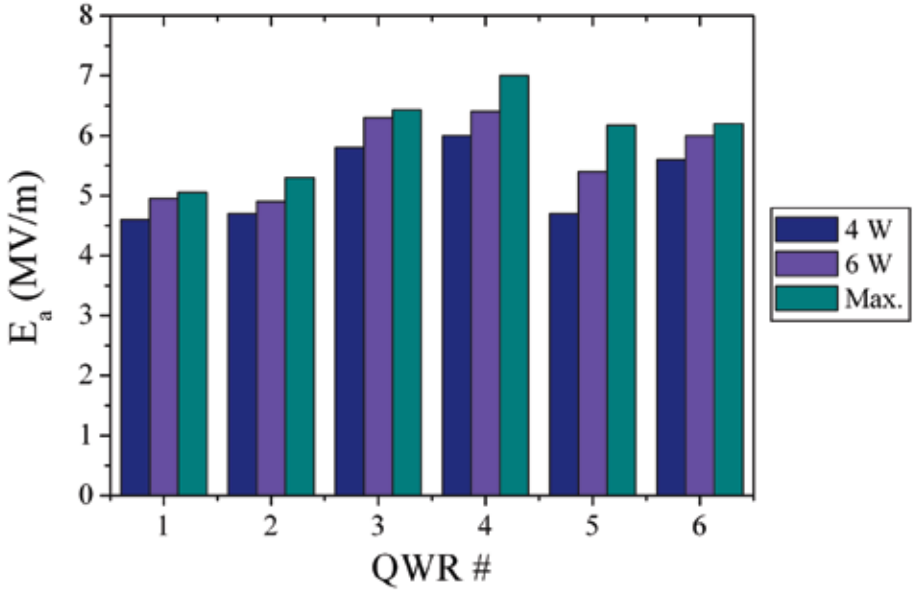

Fig. 1. CW accelerating gradients achieved in the indigenously built QWRs for the linac at different input power levels. The pulsed gradients have been ~20-25% more.

2.1.3.2 NIOBIUM LOW BETA RESONATOR

The proposed High Current Injector system at IUAC will consist of several accelerating structures including a superconducting low beta module containing niobium resonators, for which a low beta resonator has been designed and fabricated. The resonator is optimized for β=0.05 operating at 97 MHz [1]. Fabrication of the first niobium prototype has been completed. In figure 2, the niobium resonator is shown. It will be tested in the next few weeks.

Fig. 2. First prototype niobium low beta resonator built at IUAC.

Bead pull measurements have been performed on the niobium low beta resonator to measure the frequency perturbation from which several parameters could be calculated. In addition, the frequency tunability has also been measured separately. In Table 1, the results from these measurements have been summarized.

Table 1: Measured values of the parameters on the prototype niobium low beta resonator versus calculated values from CST-Microwave Studio code.

Parameter	Calculated Value	Measured Value
Frequency f	97.0 MHz	96.5 MHz
Synchronous Velocity β_0	0.051	0.051
Stored Energy U_0 (@ 1 MV/m)	26 mJ	26.4 mJ
Geometric Shunt Impedance R_{sh}/Q	650 Ω	620 Ω
Frequency Tunability Δf_{ST}	100 kHz	90 kHz

2.1.3.3 SINGLE SPOKE RESONATORS

Fabrication of the Single Spoke Resonators (β=0.22, f=325 MHz) for Project-X at Fermi National Accelerator Laboratory (FNAL) has been delayed due to the sudden and long breakdown in the electron beam welding machine. Despite this setback the project has advanced sufficiently. All the four End Walls, needed for the two resonators, have been completed. The daisy and donut ribs have been attached to the End Walls. The outer shells and End Walls have been electropolished (figure 3). Development of the spoke-to-shell collar transition has started. Once the spokes are completed they would be electropolished. After fitting the spoke to the shell the resonators would be completed by attaching the End Walls to it. This work is expected to be completed in the next few months.

Fig. 3. Clockwise from top left, setups showing the electron beam welding of (a) daisy ribs to the end wall and (b) donut rib to end wall, (c) all four completed end walls, (d) close up view of an end wall (e) electropolishing setup for the end wall, and (f) electropolishing setup for the outer shell.

2.1.3.4 SINGLE & MULTI CELL CAVITIES

Under the Indian Institutions and Fermi Lab Collaboration (IIFC), Raja Ramanna Centre for Advanced Technology (RRCAT), Indore and IUAC had jointly developed two 1.3 GHz TESLA-type niobium single cell cavities. At 2 K both the cavities achieved modest accelerating gradients of 20-23 MV/m. Based on the lessons learned from the fabrication of the first two cavities, two more *improved single cell cavities* were fabricated last year. In figure 4(b), one of the cavities is shown. In cold tests at 2 K, both the cavities achieved accelerating gradients of more than 35 MV/m, with the second improved single cell cavity (overall fourth) achieving 37.5 MV/m (figure 5). At 1.8 K the first improved single cell cavity (overall third) could achieve 40 MV/m gradient. These gradients compare very well with cavities fabricated elsewhere in the world.

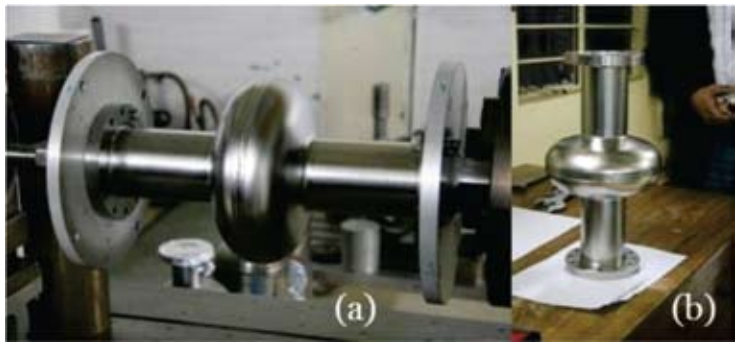

Fig. 4. (a) Setup for doing the final equator welding on the single cell cavity, and (b) one of the improved 1.3 GHz TESLA-type single cell cavities.

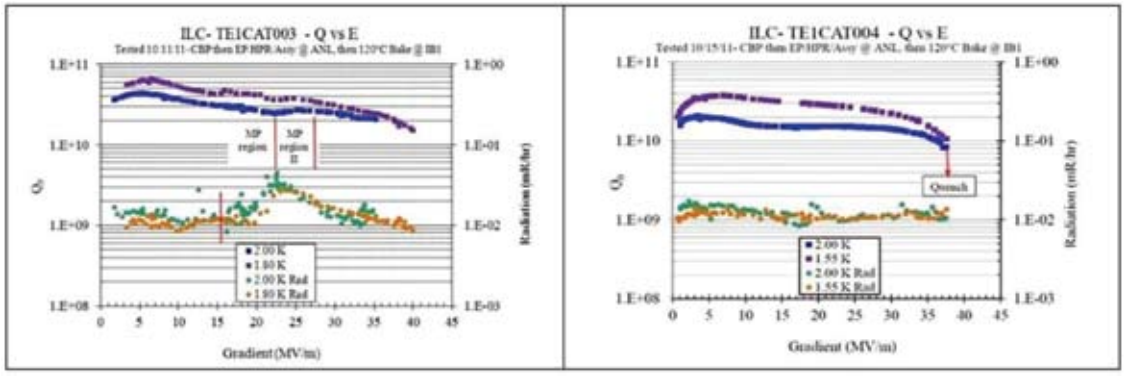

Fig. 5. 2 K test results in the improved single cell niobium cavities.

Encouraged by the performance of the single cell cavities, RRCAT and IUAC are now jointly developing a 1.3 GHz 5-cell cavity. This is the first time in India that a niobium multi-cell cavity is being made. In figure 6, one of the dumbbells is shown. The complete multi-cell cavity is expected to be ready in the next few weeks.

Fig. 6. Photograph showing a dumbbell for the 1.3 GHz 5-cell niobium cavity.

2.1.3.5 STUDIES ON THE SUPERCONDUCTING PROPERTIES OF ELECTRON BEAM WELDED NIOBIUM

For achieving high accelerating gradients in superconducting niobium resonators, apart from optimizing the design parameters it is also important to understand the influence of the various fabrication processes. With this in mind a study was taken up to understand the effect of electron beam welding on the superconducting properties of niobium materials in different joint design configurations. Controlled samples of electron beam

welded niobium materials were prepared and DC magnetization measurements were made using a vibrating sample magnetometer to determine the magnetic field for the first flux line penetration, H_p, in superconducting niobium. The measurements were made at 4 K and 2 K, which are the temperatures at which superconducting cavities usually operate. In figure 7, results from the measurements made at 4 K are shown. In the first approximation the field for first flux line penetration can be estimated as the field H_p where the virgin leg of the isothermal M-H curve deviates from its linear dependence, as shown. The study indicated that there is no significant difference between butt joint and step joint electron beam welded and electropolished niobium materials as compared to the as-received electropolished sample; the butt joint is only marginally better. Details of this study can be found in reference 2.

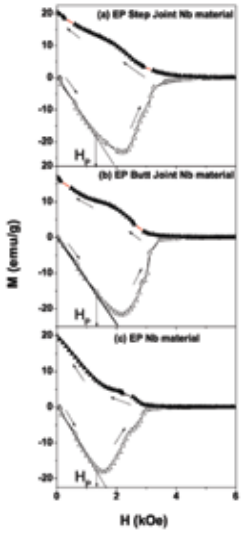

Fig. 7. Isothermal M versus H plots of (a) electron beam welded and electropolished niobium step joint (top), (b) electron beam welded and electropolished niobium butt joint (middle), and (c) electropolished as-received niobium (bottom), starting from the zero field cooled state at 4 K.

2.1.3.6 FACILITY UPGRADE

The SRF infrastructure at IUAC is nearly a decade old. Over this period the facilities have been extensively used for fabricating niobium resonators. The present control system hardware on the electron beam welding machine is obsolete. Several systems in the highly acidic environment of the surface preparation lab (used for electropolishing) have got corroded. Similarly some of the hardware components, vacuum pumps and other items in the high vacuum furnace have started to malfunction. It is essential to maintain the infrastructure in top condition in order to continue fabricating superconducting niobium resonators. The non-availability of any key component in these crucial facilities is a serious issue. In view of this we have decided to upgrade the facilities. Keeping in mind the ongoing works and immediate commitments, the upgradation work will be spread over two years.

For the electron beam welding machine a new control system running on a modern PC, operating system and commercially available CNC and PLC controls is being procured. The new system will also have additional features in the control program, like recording of real time welding parameters, digital video recording of the entire welding process etc. In addition, the electron gun will be sent to the factory in France for replacing the gun oil and overhauling. The entire machine, including the vacuum system and other controls, will also be overhauled to ensure smooth operation and service for several years to come.

Upgradation of the surface preparation laboratory and high vacuum furnace will also be gradually taken up. In the chemical lab, the fume hood and its drainage system will be re-furbished. A new clean room with separate entrance is being planned along with a high pressure rinsing system inside it. In the high vacuum furnace the controls and electrical systems will be refurbished and the entire machine, including the vacuum pumps, will be overhauled. Some civil and structural changes in these facilities will also be carried out to reduce the dust level.

REFERENCES

[1] Prakash N. Potukuchi and Amit Roy, PRAMANA-Journal of Physics, Vol. 78, No. 4, April 2012, p565-584

[2] Prakash N. Potukuchi, L.S. Sharath Chandra, M.K. Chattopadhyay, D. Kanjilal, Amit Roy and S.B. Roy, Phys. Rev. ST Accelerators & Beams 14, 122001 (2011)

2.2 HIGH CURRENT INJECTOR (HCI)

2.2.1 HIGH TEMPERATURE SUPERCONDUCTING ECRIS -PKDELIS AND LOW ENERGY BEAM TRANSPORT (LEBT)

G.Rodrigues, P.S.Lakshmy, Y.Mathur, R.Ahuja, U.K.Rao, A.Mandal, D.Kanjilal & A.Roy

A. EXPERIMENTS WITH 18 GHZ HIGH TEMPERATURE SUPERCONDUCTING ECR ION SOURCE, PKDELIS

(a) Measurements of plasma potentials of heavy ions and influence of the energy spread on the longitudinal optics of the High Current Injector

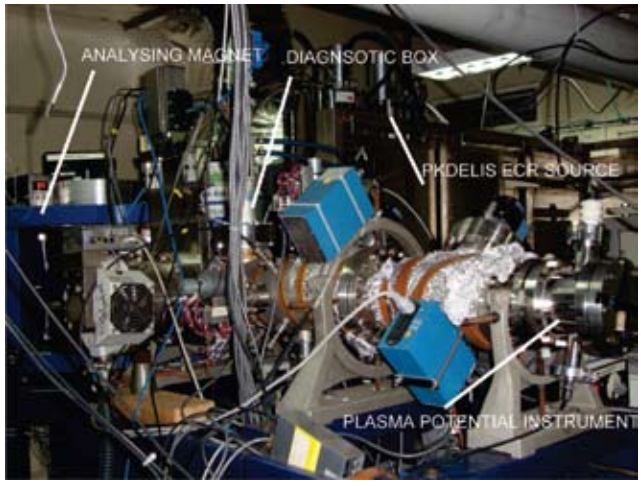

Fig. 1.View of the plasma potential measuring instrument coupled to the low energy beamline

Plasma potentials for various heavy ions have been measured using the retarding field technique in the 18 GHz High Temperature Superconducting ECR ion source, PKDELIS [1]. The ion beam extracted from the source is decelerated close to the location of a mesh which is polarized to the source potential of 6 kV and beams having different plasma potentials are measured on a Faraday cup located downstream of the mesh (figure 1). The influence of various source parameters viz., RF power, gas pressure, magnetic field, negative DC bias and gas mixing on the plasma potential is studied. The study helped to find an upper limit of the energy spread of the heavy ions which can influence the design of the longitudinal optics of the High Current Injector being developed at the Inter University Accelerator Centre. It is observed that the plasma potentials are decreasing for increasing charge states and a mass effect is clearly observed for the ions with similar operating gas pressures. In the case of gas mixing, it is observed that the plasma potential minimises at an optimum value of the gas pressure of the mixing gas and the mean charge state maximises at this value. Considering the worst possible case of the heaviest ions being accelerated through the high current injector ($^{238}U^{40+}$), an energy spread, ΔE, of 0.11 % would result in a corresponding phase spread, $\Delta\phi$ given by the equation $\Delta v/v = \Delta\phi\beta\lambda/\pi h L_{drift}$ at the entrance of the RFQ (where L_{drift}, distance of 4.0 m from the MHB, considering the length of the MHB and the harmonic number, h = 4). The model calculations by TRACK using the value of energy spread from the ECR source showed that a significant phase spread $\Delta\phi$~ +/- 22.5o arising from the energy spread, would need to be accommodated by the RFQ phase acceptance ellipse. The calculations show that the transmission through the RFQ is reduced by 16 % due to the energy spread in the beam. The deterioration in the energy spread after the RFQ is minimal and it is expected that the final injection into the main linac would not pose problems for phase matching through the next accelerating elements of the DTL. Since adjustment of the source parameters like gas pressure and rf power play a critical role in deciding the energy spread of the ion beams extracted, it would be necessary to optimise these parameters as determined from the present study for good transmission of the ion beams through the high current injector. It is shown that tuning of the ion source parameters like dc bias and gas mixing can bring about a reduction of the energy spread of the ions. The experimental results show that the energy spread of the ions determined from the plasma potential measurements is a determining factor for the resultant time width of the beam bunches that would be accelerated further by the high current injector.

B. MAINTENANCE ACTIVITIES

(a) In this year we faced one major problem with the 1.8kW, 18GHz Klystron microwave amplifier. Its 9KV high voltage power supply was not getting on and also amplifier was not coming to the ready state. We diagnosed and analyzed that it was due to one 12V relay RE4 and electronic components diode1N4148 (D8) & resistor (R14) in its CD control unit. These components got damaged due to the high voltage spark in the source chamber during one of the run. Relay RE4 in it was a special type of imported relay and it was also not readily available. So we had modified the part of the CD control unit board and replaced this relay and other components with the locally available components (as shown in figure2). It is now working properly and is being used regularly.

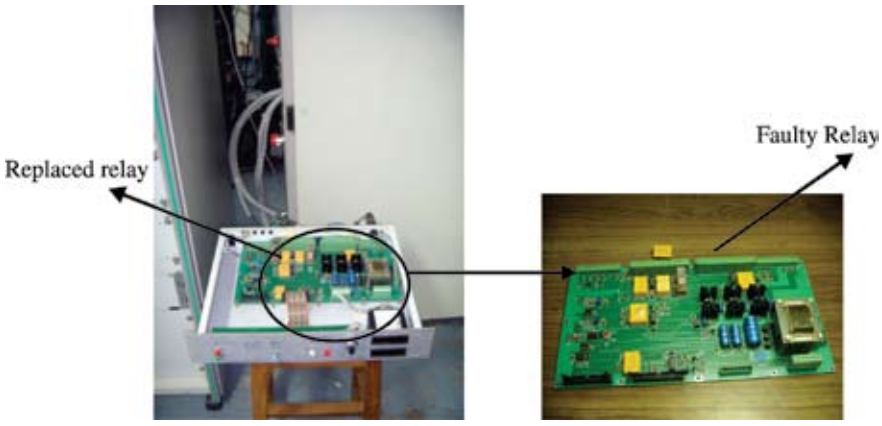

Fig. 2. CD control unit of Klystron Amplifier

(b) Control System Upgradation : The PKDELIS ECR ion source control system has been upgraded. The remote monitoring set-up for source room has been added. It is continuously logging the source room temperature using the modbus module on the control computer. It will be used to study the effect of source room temperature on various beam tuning parameters.

A remote temperature monitoring set up to study the needle valve temperature on beam tuning during the operation has also been added.

C. DEVELOPMENT OF 2.45 GHZ ECR SOURCE

(a) A 2.45GHz Electron Cyclotron Resonance (ECR) source has been developed at IUAC [2]. It provides the high intensity beam of singly charged ions for various material science experiments and related applications. Permanent magnet rings are used to achieve the required ECR magnetic field (875 gauss). This source helps in reducing the total time related to the ion implantation and irradiation experiments using singly charged ion beams when compared to multiply charged ions. Figure 3 shows the schematic of this source with beam extraction system.

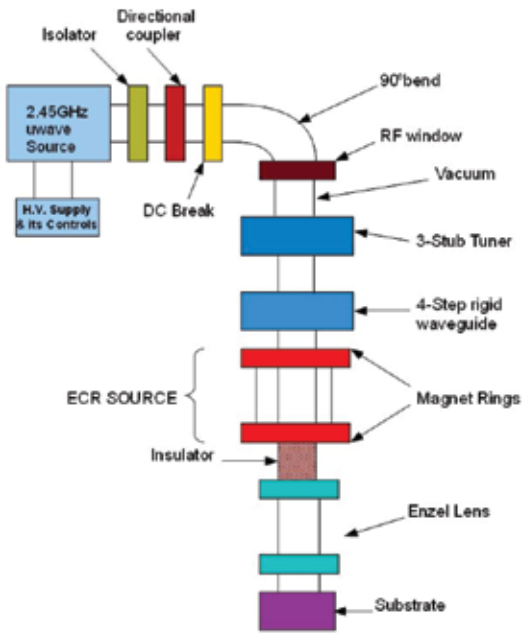

Fig. 3. Schematic of 2.45GHz ECR source, RF injection and beam extraction system

This source has been installed in the old LEIBF (Low Energy Ion beam Facility) source room along with its beam extraction system. The ECR source is operated at high potential (max. 15 kV) to extract the beam and focus the beam in combination with an Einzel lens. A local control system has been developed and installed to test this ECR source set-up. This control system includes the controls and monitors for microwave power, gas flow, extraction and einzel lens power supplies as well as interlocks based on PLC's. The PLC (Programmable logic controller) based interlock system has been developed and installed for this set-up. Figure 4 shows the installed view of this source along with its control system.

The first ion implantation test experiment has been carried out successfully by operating the source at 5 kV extraction voltage for singly charged nitrogen beam. RF power of 38 W was utilized for the implantation of N^+ on a silicon substrate for formation of SiN. Forced air cooling was maintained to keep the source and the magnet rings below 40 degree Celsius to avoid demagnetization of the permanent magnets. Due to irregularities in the forced air-cooling especially at higher RF power levels, it was decided to upgrade the system using a double walled plasma chamber with water cooling.

Fig. 4. Installed view of (A) 2.45GHz ECR source, (B) Control System (C) Dual Gate Valve Interlock

(b) Dual gate valve interlock has been developed for the 2.45GHz ECR Source system to control the operations of two gate valves manually as well as automatically. It has an LED indicator to verify the gate valve positions. Figure 4 (C) shows the photo of the interlock box.

(c) Part of the room 117 has been allocated for development of the 2.45GHz ECR source and maintenance area for the 18 GHz HTS ECR source and related ion sources. It has also been decided to shift the 2.45GHz ECR source setup from the old LEIBF source room to this area. So accordingly a layout has been designed as shown in figure 5 and work is underway to install a new compact beamline.

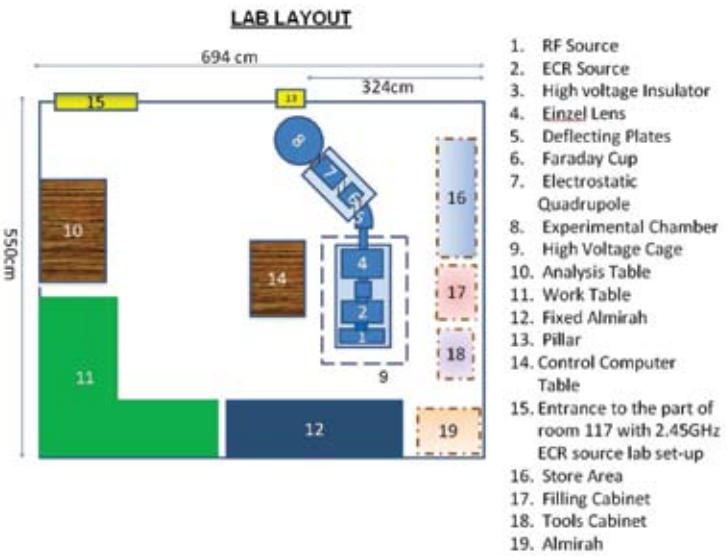

Fig. 5a. Layout designed for development of 2.45GHz ECR source system and maintenance area for the 18 GHz HTS ECR source and related ion sources

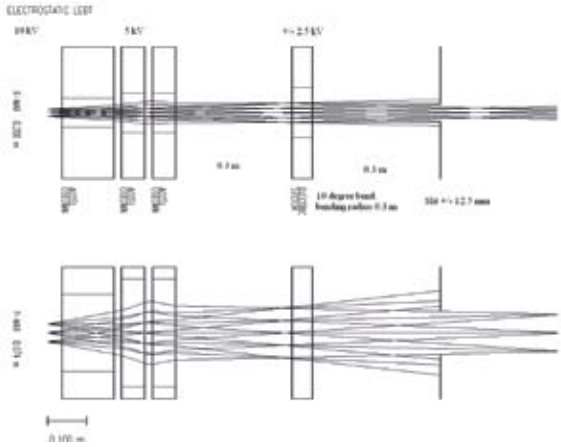

Fig. 5b. Optics for the compact beam-line depicting a 2.45 GHz ECR source, Einzel lens and a 10o electrostatic deflector

(d) Design of a new water cooled plasma chamber and a microwave injection line for 2.45GHz, permanent magnet ECR ion source : A water cooled plasma chamber for a permanent magnet based ECR ion source operating at 2.45GHz has been designed. The plasma chamber is a double walled stainless steel cylindrical cavity having an inner diameter of 90mm and length of 101mm. The dimensions of the resonant cavity have been chosen to excite the TE_{111} dominant mode at 2.45GHz. The actual length of the plasma chamber has been kept 135mm in order to accommodate the magnet structure. The positions of injection and extraction side magnet rings have been adjusted to coincide the magnetic field resonance point with microwave launching position at the injection side and position of plasma electrode at the extraction side respectively. The simulated magnetic field distribution (using PANDIRA) for an inner gap of 105mm between magnet rings is shown in Fig. 6. Additional ports have been provided on the chamber wall for Langmuir probe plasma diagnostics. Fig. 7 shows the water cooled chamber in which cooling water can flow all over the chamber through equally spaced ribs in between the walls and also cold and hot water are separated by a closed rib.

The microwave injection line has been designed to couple microwave power from a 1.2 kW magnetron into the plasma chamber using a four-step ridged waveguide. The RF window has been placed after a 90^0 bend as shown in Fig. 8 in order to protect the window from backstreaming electrons coming from plasma. The ridged waveguide effectively couples microwave power into the plasma chamber by progressively matching the impedance and concentrates the electric field at the centre of the plasma chamber. Fig. 9(a) shows the simulated electric field contours (using CST Microwave Studio) for TE_{111} mode inside the plasma chamber using a normal waveguide and Fig. 9(b) shows the field contours while using a four-step ridged waveguide to couple power and it shows that ridged wave guide structure can enhance the electric field at the centre of the plasma chamber by a factor of 1.5 as compared to a normal waveguide.

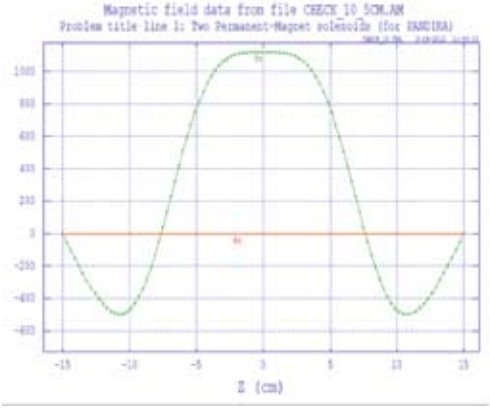

Fig. 6. Magnetic field distribution along the axis of plasma chamber

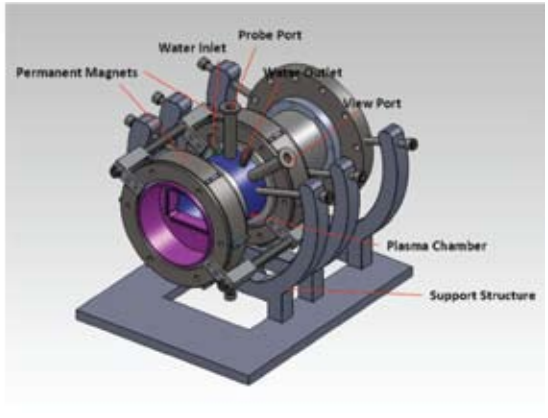

Fig. 7. View of magnet structure with new plasma chamber

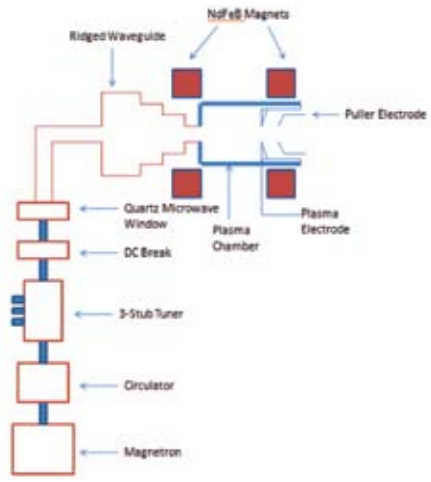

Fig. 8. A schematic view of the 2.45 GHz ECR with microwave injection system

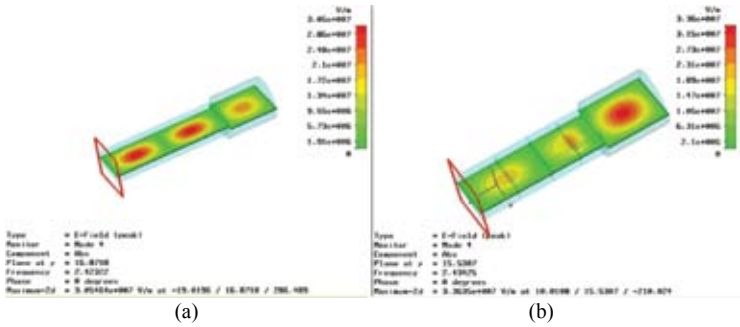

(a) (b)

Fig. 9. Simulated electric field contours; (a) Power coupled using normal waveguide (b) Power coupled using ridged waveguide

REFERENCES

[1] G.Rodrigues, R.Baskaran, S. Kukrety, Y.Mathur, Sarvesh Kumar, A.Mandal, D.Kanjilal and A.Roy, Rev.Sci. Instrum.83,033301(2012)

[2] Y.Mathur, G.Rodrigues, R.Ahuja, U.K.Rao, N.Kumar, P.S. Lakshmy, D.Kanjilal & A.Roy, Proceedings of the Indian Particle Accelerator Conference, IUAC, New Delhi, 2011

2.2.2 RADIO FREQUENCY QUADRUPOLE ACCELERATOR

HIGH POWER RF TEST ON THE 1.17m MODULATED PROTOTYPE RFQ ACCELARTOR: This year Re-plating (by copper) of the inner wall of RFQ chamber made of Stainless Steel material was done from RRCAT, Indore. Plating was done to improve the quality factor. The original base plate made of stainless steel was replaced by base plate made of copper material. It was done to improve the quality factor as the magnitude of current is large on the base plate. Power coupler made of copper tube of diameter 6 mm and length 500 mm was used to couple power in the cavity. The coupler was optimized for critical coupling to minimize reflected power. Low power RF test were done to measure the resonant frequency, Quality factor, Shunt Impedance; Power required, Longitudinal & Transverse Electric field profile, Quadrupole symmetry etc. The measured resonant frequency and Intrinsic quality factor of the cavity is 53.02MHz and 4312 respectively. The 35kW high power amplifier was characterized at different frequencies to check its bandwidth. The amplifier has bandwidth of ±1MHz. The amplifier attenuation is minimum at 48.36MHz. The resonance frequency of the modulated RFQ is 53MHz. To bring resonance frequency within the frequency bandwidth of RF amplifier, some of the modulated vanes were replaced by unmodulated vanes. This process brought resonance frequency to 48.33156 MHz. The vacuum leak testing of RFQ chamber was done to maintain the low pressure of 10^{-6} to 10^{-7} Torr during high power. Low pressure is required to remove moisture from chamber which is essential to avoid electric spark in the presence of very high electric field in high power condition. Water flow and air flow were maintained to ensure efficient removal of heat generated in vanes and power coupler during high power run. High power tests were done to check the frequency and temperature stability. During test, power was fed in small steps as there was huge degassing with rise in temperature of cavity.

Low power conditioning was done for more than 72 hours to take care of degassing and sudden fluctuation in vacuum. There was a shift in resonance frequency of cavity with increasing power and therefore the signal generator frequency was tuned accordingly to minimize the reflected power. In small steps we fed 18kW power in the cavity but were unable to go above as there was huge power reflection above 18kW.

Local heating was found in certain areas of the cavity walls. Marginal rise in temperature of water is also

observed with increasing power. The water temperature as well as resonance frequency were measured with power for further analysis. We also observed a marginal decrement in the coupling coefficient as well as quality factor with increasing power.

Design of the final RFQ

After completion of the prototype RFQ, the final RFQ has been designed using Solidworks, a design and drawing software keeping the following basic requirements in as follows:

- Total Length of Vanes : 2536mm
- Aperture :12 mm
- Inner Dimensions of Chamber : 620(W)x500(H)x2576(L) mm

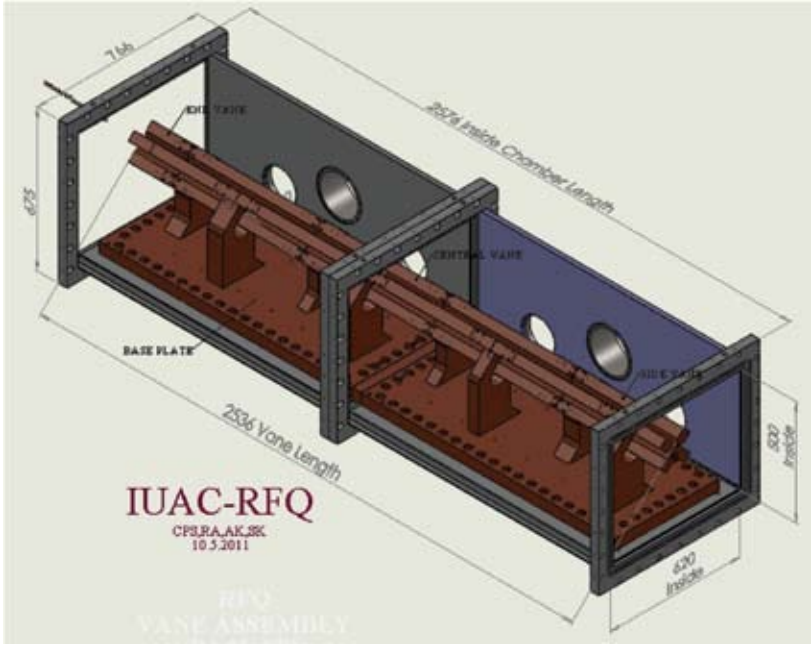

Fig. 1. IUAC RFQ design

Mechanical Design :

Final RFQ will have two copper plated vacuum chambers with water cooling provision all around. There will be two solid copper base plates which will hold eight nos. of vane supports. These vane supports will hold twenty nos. of vanes. Water will flow into vanes through vane posts. The chambers will be kept on a stand which will have the provision for alignment in all the three axis. All design and drawing work has been done using solid works. The chambers are designed to hold vacuum up to $1x10^{-8}$ torr. Both the chambers will be assembled together to make one single tank. The bottom plates of both the chamber have been machined perpendicular to the side flange to an accuracy of 0.25º, so that both the chambers are straight after assembly. The bottom plate is the back bone of the chambers. The chamber has been designed in such a way that the bottom plate can be machined after welding. The bottom plate will hold the copper base plate. The base plates will be aligned with the help of portable co-ordinate measuring machine (CMM) as was done in the prototype RFQ.

The pressure, static and buckling design analysis was also done by using solid works.

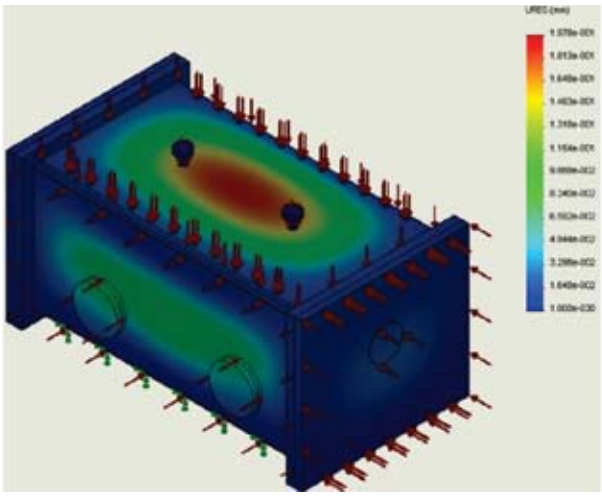

Negative pressure on wall of UHV Chamber
Max. Deformation : 0.19 mm

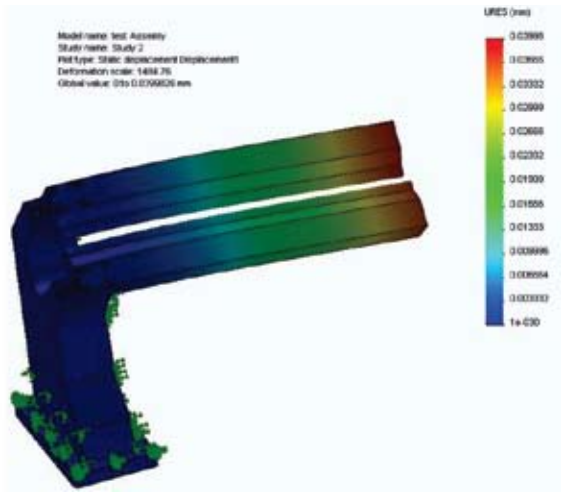

Bending of side vanes due to self weight
Max. Deformation : 0.039 mm

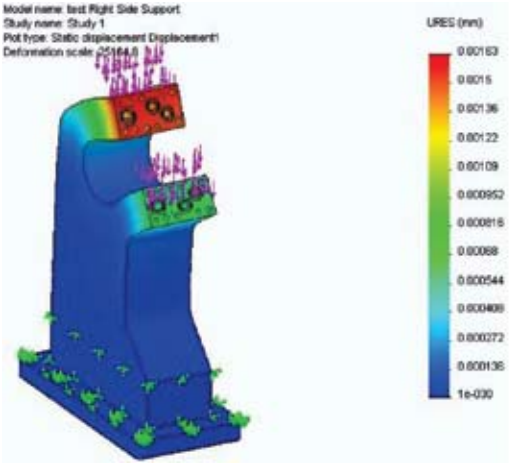

Bending of Vane post due to load of vanes on it
Max. Deformation : 0.0016 mm

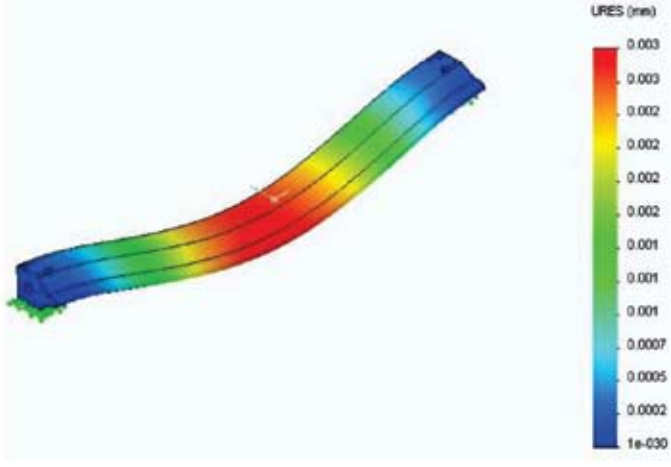

Bending of Central Vane due to its own weight
Max. Deformation : 0.003 mm

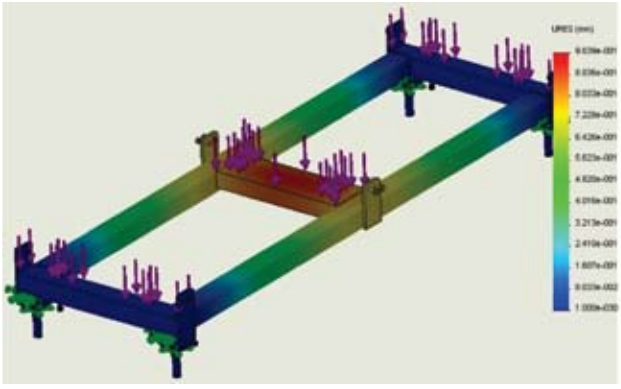

Bending of upper frame .
Max. Deformation : 0.5 mm

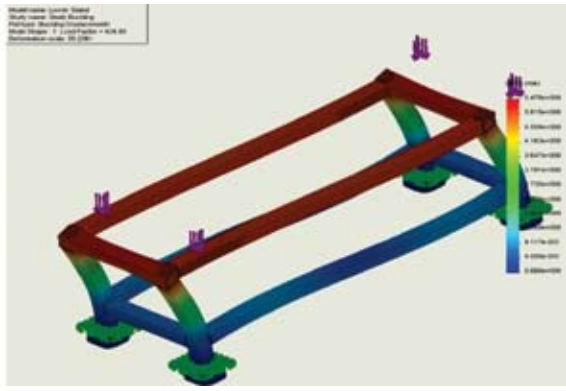

Max. Deformation due to buckling in stand :
0.12 mm

Fig. 2.

Present Status : The design and drawing work of all the components is over. Vacuum chambers have been successfully fabricated within the specified tolerance limits at M/s. Vacuum Techniques, Bangalore. The chambers have been sent to RRCAT, Indore, for copper plating. OFHC copper material, required for vanes etc., has been imported. Fabrication of vanes, vane posts and base plates is going on at Indo German tool Room, Ahmedabad.

2.2.3 DESIGN VALIDATION OF PROTOTYPE DRIFT TUBE LINAC RESONATOR & HIGH POWER RF TEST

R Mehta, R V Hariwal, J. Sacharias, Y Mathur, U K Rao, Rajesh Kumar, B P Ajith Kumar

The High Current Injector (HCI) project at Inter University Accelerator Centre uses a Radio Frequency Quadrupole (RFQ), Drift Tube Linac (DTL) and low beta superconducting cavities to accelerate heavy ions having $A/q \leq 6$, from the high temperature superconducting electron cyclotron resonance ion source (HTS-ECRIS called PKDELIS) to the existing superconducting linear accelerator (SC LINAC). The required output energy of the DTL is decided by the minimum input velocity ($\beta = 0.06$) required for the existing superconducting LINAC. The beam dynamics and generation of the drift tube geometry is done using the LANA code [1]. A full scale prototype resonator has been fabricated [2] for validating the design. Frequency, voltage profile measurements and high power RF test have been done on a full size prototype resonator.

High Power RF Test, Results and Analysis

Prototype resonator with a water cooled power RF coupler was assembled. A tube based 10 kW RF amplifier was used to power the resonator. Before starting high power test the input power coupler was optimized using network analyzer. Network Analyser (NA) was used to optimize the coupling coefficient close to critically couple condition. For this measurement NA is connected to drive the low power through coupler. The input port voltage reflection coefficient S11 refers to the signal reflected at a given port for the signal incident at the same port. Using this S11 data from NA coupling coefficient was measured as

$$\beta = 0.923$$

Intrinsic quality factor was measured using NA and was found to be 8500. For high power test water connections were made to cool the various parts of the cavity. Due to degradation in vacuum from $5.0X10^{-6}$ torr to $2.3X10^{-4}$ torr even at low power levels, input power was ramped at very slow rate, maintaining the vacuum better than $5X10^{-5}$ torr. After initial conditioning at ~20 Watts for 18-20 hrs, we could jack up the power at higher ramp rate. We observed that at around 60 - 70 watts input power vacuum deteriorated drastically, pickup signal collapsed and pickup signal was not increasing with input power. This was clear sign of occurrence of multipactoring. To check this resonator was opened and dark black spots were seen only on the exit flange (see figure below).

Fig. 1. Multipactoring Effect on the Exit Flange

Detailed calculations were carried out using electric field distribution from CST Microwave Studio to correlate the experimentally observed fact. It was found that multipactoring condition is met around the same place where we observed the multipactoring during experiment. Resonator was cleaned and assembled again for the high power rf test. This time, to avoid, multipactoring we started with 200 watts input power and no further sign of multipactoring was observed. This test continued for ~ 100 hrs with maximum power of 6 kW. To check the frequency and temperature stability of the resonator, 4 kW input power level was maintained for 20 hrs continuously. Observed frequency shift was ±10 kHz (Fig 2) without a frequency tuner installed to correct the frequency drift. Result also shows that the coupling coefficient β changes to ~0.5 around 3kW from initial value of 0.923. Beyond this power level β remains almost constant (Fig 3). This implies that we need to optimize the β to ~ 1.8 at extremely low power (few mW) to have critically couple state at high power. Temperature measurements on the outer surface of the tank shows that end plates and ridge-tank joint area are getting hot and require better cooling system. Temperature measured at ridge top was ~ 55 C at 6 kW.

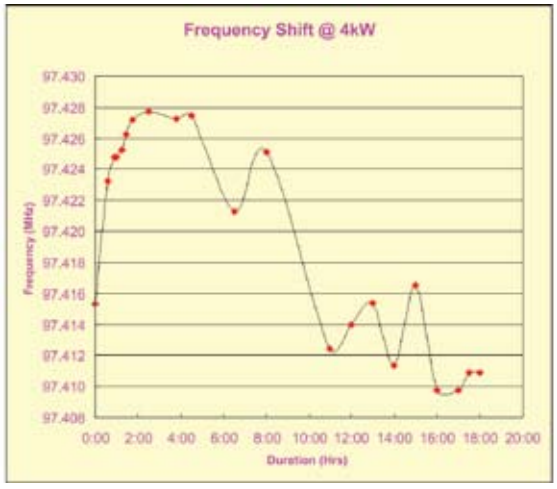

Fig. 2. Frequency shift at 4 kW

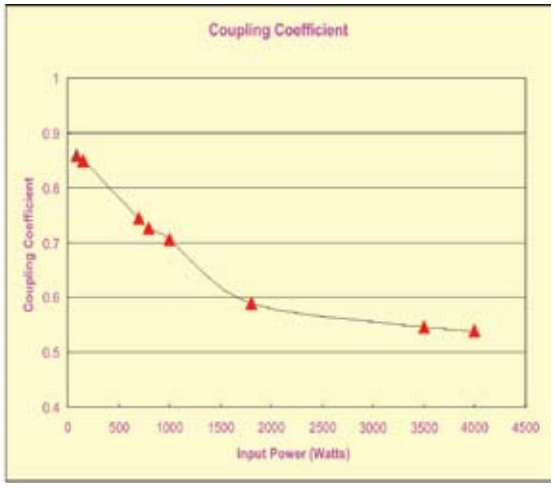

Fig. 3. Coupling Coefficient variation with Input Power

Temperature profile shows that end plates and ridge-tank joint area is getting hot. Temperature measured at ridge top was ~ 55 C at 6 kW (Fig 4). For tested power range of 0 - 6 kW the frequency change was calculated to be 3.9 kHz/ βC (Fig5). Figure 6 shows effect of heating on end plates at different power levels

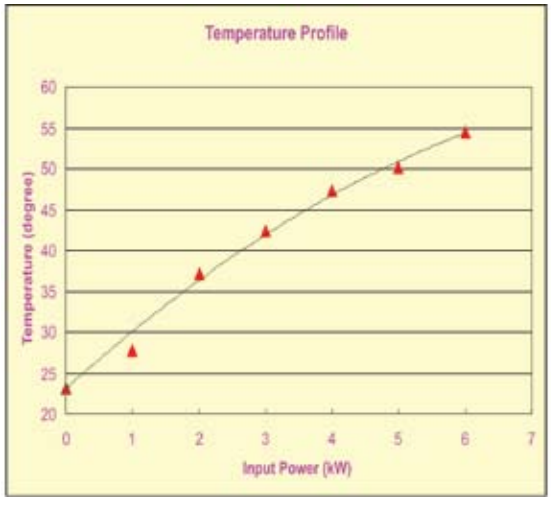

Fig. 4. Temperature Profile at various Input Power Levels

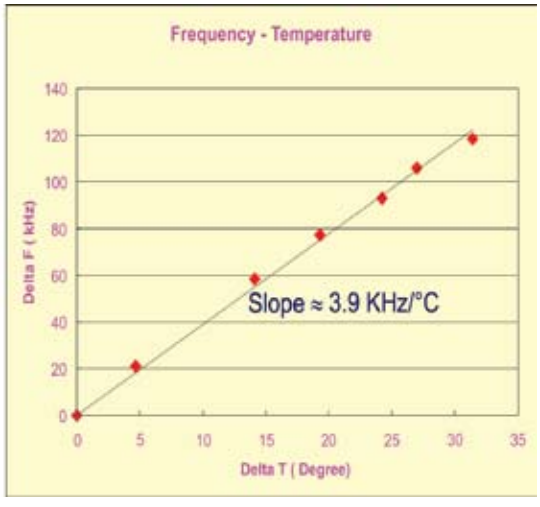

Fig. 5 Frequency and Temperature variation at Various Input Power Levels

Fig. 6. Heating Effect as Seen on End Plates at 3 kW, 4 kW and 6 kW

Current Status : After validating the design of resonator with high power test it was observed that cooling efficiency needs to be improved around the ridges. This prompted us to undertake some modifications. At present work on increasing cooling efficiency of the resonator is going at vendor's site. To improve the quality factor of the resonator copper plating on the aluminium stems and better RF contact by having enhanced surface finish is being carried out.

REFERENCES

[1] "Beam Optics and Resonator Design for the 97 MHz DTL at IUAC", Indian Particle Accelerator Conference - 2009, RRCAT, Indore, India.

[2] "Mechanical Design, Fabrication and Initial Tests on Prototype Drift Tube Linac at IUAC", by J Sacharias, R Mehta, Ajith kumar B P and R V Hariwal, Indian Particle Accelerator Conference - 2011, InPAC2011, IUAC, New Delhi, India

2.2.4 BEAM TRANSPORT SYSTEM

A.Mandal, Rajesh Kumar, S.K.Suman, Mukesh Kumar and Sarvesh Kumar

Beam Transport System laboratory takes care of regular maintenance, design and development of Accelerator beam Transport System. This year the major thrust has been given for installation of facility and simulation of beam optics for HCI for various options. Different beam transport elements viz. quadrupole magnets, electrostatic quadrupoles, beam diagnostic elements etc are being developed for LEIBF and HCI. Power supplies for different magnets have been indigenously developed. Other than power supplies the group is actively involved in development of equipments for the others lab at IUAC. Details of development activities are summarised below.

2.2.4.1 BEAM OPTICS OF HIGH CURRENT INJECTOR

Sarvesh Kumar & A Mandal

The beam optics of high current injector is being divided into three different energy regime parts as follows with input parameters given in table-1.

I. Low energy beam transport section (LEBT)

II. Medium energy beam transport section, RFQ to DTL (MEBT)

III. High energy beam transport section (HEBT)

Table-1 : Ion optical parameters of different sections

Parameters	LEBT	MEBT	HEBT
Emittance(ε_x & ε_y) π mmrad, ε_z (π deg. keV)	50, 9	15, 176	9, 351
Mass to charge ratio (A/q)	6	6	6
Max. Magnetic rigidity (Bρ) Tm	0.09	0.36	1.15
Initial energy (E) keV/u	5	180	1800

I & II. Low and Medium energy beam transport section (LEBT and MEBT)

The transverse beam optics of LEBT section has been done using TRANSPORT code earlier. The beam parameters as obtained by TRANSPORT code before multiharmonic buncher are used in the code TRACE3d to study the longitudinal beam optics. The magnetic quadrupole doublet after the source has been tested experimental after fabrication and results of horizontal field mapping and excitation studies are shown in fig. 1a.The beam has been tracked in the multiparticle beam dynamics code TRACK and obtained the beam parameters after RFQ which are utilized in TRACE 3D again to matching parameters of DTL design. The beam dynamics is shown in the fig. 1b for both LEBT and MEBT section.

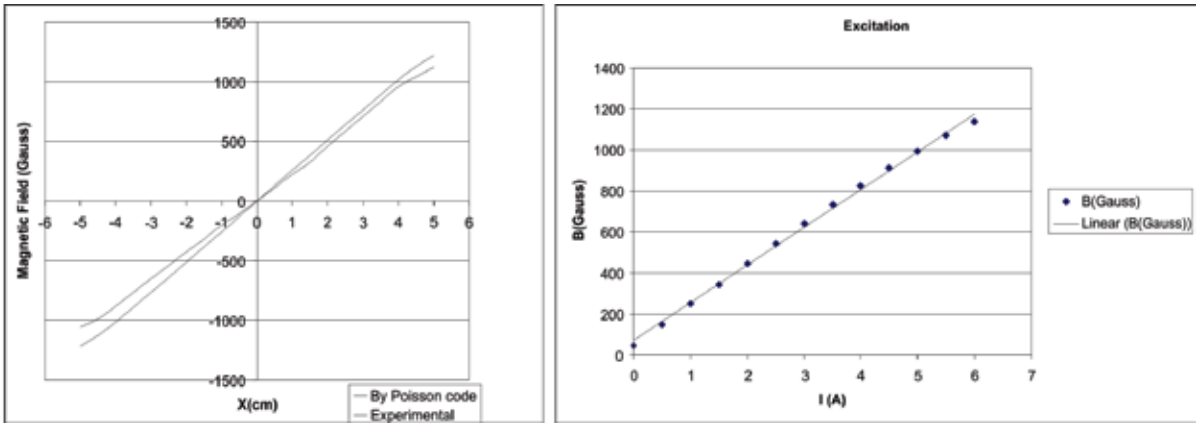

Fig. 1a. Field mapping and excitation of MQD

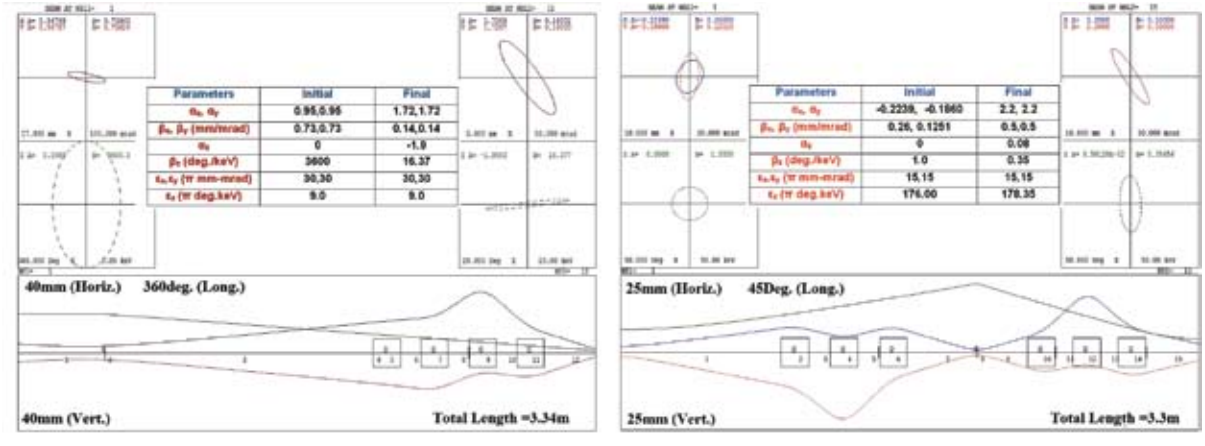

Fig. 1b. Beam dynamics simulations of LEBT and MEBT using TRACE 3D code

III. High energy beam transport section (HEBT)

The beam exiting the DTL is transported to super buncher through HEBT section by the four achromatic bends of 90deg. Each bend consists of two 45-45 deg. magnets identical in terms of edge angles (24deg.) and bending radius (850mm). The first three bends are same in terms of magnetic quadrupole configuration in the achromats but the last achromat has been optimized to accomodate matetial science beam line of existing pelltron in terms of quadrupole postioning. The beam optics using code TRACE3d of full HEBT section is shown in fig. 1c. and magnets requirements are in table-2. All the magnetic field gradients of quadrupoles in this secton are less than 17T/m. The layout of full HCI is shown in fig. 1d according to design-2 option of HEBT section.

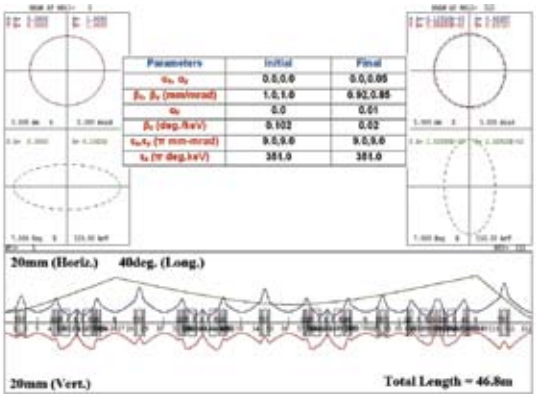

Fig. 1c. Transverse and longitudinal beam optics of HEBT section by TRACE3D

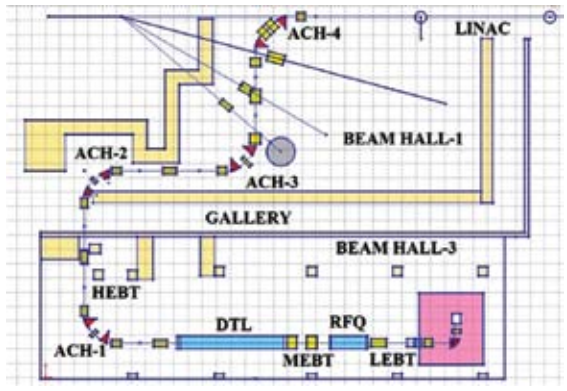

Fig. 1d. Layout of full HCI of HEBT section (1 Sq. Box = 1m x 1m)

Table-4: Magnet requirements in HEBT section of HCI

Components	Number
Magnetic Quadrupoles of effective length 106mm	12
Magnetic Quadrupoles of effective length 159mm	4
Magnetic Quadrupoles of effective length 212mm	13
45deg. Bending Magnets of radius 850mm	8
Magnetic Quadrupole triplets	4

2.2.4.2 Multi Harmonic Buncher (MHB) Electronics for HCI

Rajesh Kumar, A.Sarkar, S.K.Suman, Mukesh Kumar, A.Mandal

A new control electronics for the generation, control and locking of the saw-tooth voltage has been designed for HCI buncher. The new design is based on the existing design but with modified circuits and new components so that it can handle problems associated with the old design. The old design has several limitations like difficult debugging with several NIM modules, specially wired NIM bin, many interconnecting cables and obsolete components.

The new design has advanced features like programmable components, marrow-band low-loss readymade filters, changed modularity, in built power supply, improved front and back panels. The new design will have improved stability as well as help in easy operation and maintenance.

The design is complete which includes circuit design with modifications, cabinet with front and back panel design, wiring and layout details. The panels and pcbs are already made. All the components have been

ordered. The assembling will start as soon as we receive the components. This will be followed by the testing of the circuits.

2.2.4.3 Power Supply for HCI Steerer and low power Quadrupole Magnets

Rajesh Kumar, S.K.Suman, Mukesh Kumar, A.Mandal

For the upcoming HCI facility, we planned to develop a few low watt (~300W) power supplies for steerer magnets and low power air cooled quadrupole magnets. The design is complete which includes circuits (control and power section), cabinet (modularity, front and back panel, module placement) and wiring and layout details. This is a linear current regulated power supply having current stability within 100PPM. Design implementation is in progress.

2.2.4.4 Fabrication of Magnetic quadrupoles for LEBT section of HCI

Sarvesh Kumar, S.K.Saini, A.Mandal

The magnetic quarupoles are required in LEBT section for transverse matching the beam into radio frequency quadrupole (RFQ). The design has been prepared using the codes like POISSON and OPERA 3D. It is an air cooled quadrupole and required to produce a peak field of 0.15T by the excitation current of 6amperes. It is designed for beam of energy 8keV/u to provide sharp focus into RFQ. Fig. 4a shows the magnetic field lines in 2D using POISSON code for 1/8th geomtry and its 3D layout using solidworks.

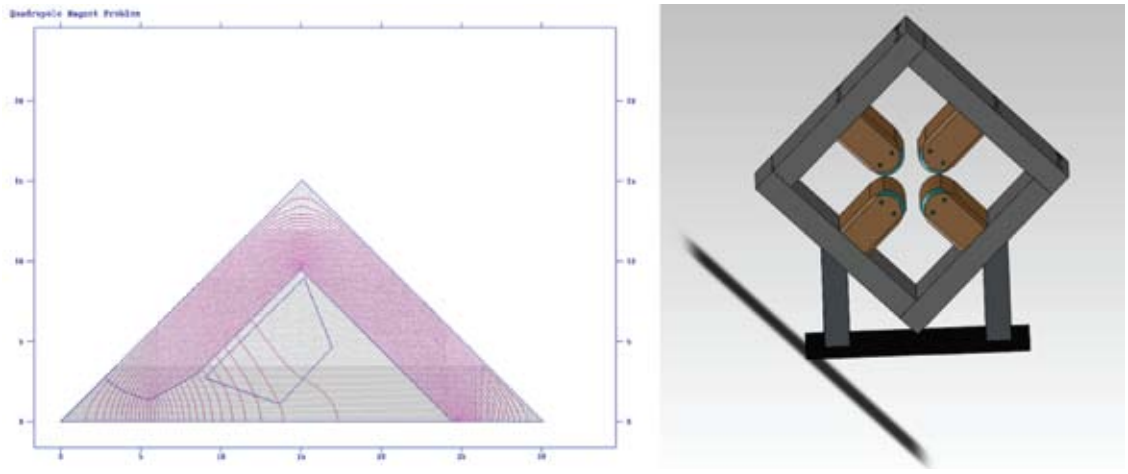

Fig. 4a. Magnetic field lines in 2D by POISSON code and full geometry in 3D using Solidworks

2.3 CRYOGENICS

T.S.Datta, J.Chacko, A .Choudhury, J. Antony, M. Kumar, S. Babu, S.Kar, D.S. Mathuria, R.N.Dutt, P. Konduru, R.G. Sharma and A. Roy

In this academic year, for the first time, the beam was accelerated through the two LINAC cryomodules with sixteen resonators. The thermal performance test of LINAC-III cryomodule without any resonators had also been done at 4.2K. The new helium refrigerator of 900W refrigeration capacity is installed and commissioned. The helium distribution system to connect with existing cryo-network is planned, designed and the order is placed to M/S A.S. Scientific. It is expected to be at IUAC site by July 2012. In the coming academic year, it is expected that full LINAC with twenty four resonators would be tested with the new refrigerator. For HYRA superconducting quadrupole magnet, all the coils are independently tested at 4.2K and mounted in the magnet assembly.

2.3.1 CRYOGENIC FACILITY

I. LIQUID HELIUM PLANT

The helium plant was operated for six times in this academic year. These runs consists of two-month long close-loop run for LINAC beam acceleration and five off-line runs for testing the LINAC-II cryomodule and superconducting quadrupoles. The approximate running hour is 1600hrs which corresponds approximately 144000 L of LHe production. Fig.1 shows the yearly LHe production.

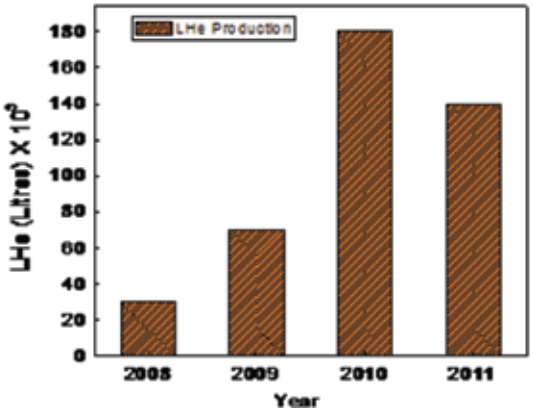

Fig. 1. Yearly LHe Production

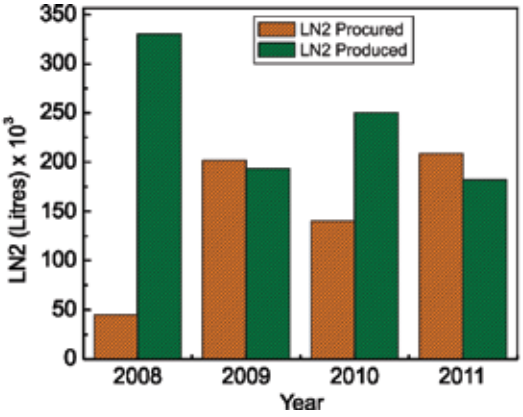

Fig. 2. Yearly LN2 Inventory

II. LIQUID NITROGEN PLANT

In this academic year, total in-house production of LN2 was 1,82,000 L. LN2 procured from outside vendor was 2,08,000 L. Fig.2 shows the yearly LN2 production and amount of procurement. A remote monitoring system has been designed and developed to monitor the LN2 level and pressure of the four LN2 storage vessels situated at two different locations at the lab complex. The system is based on the high precession Field-Bus ADCs. The outdoor hardware complies with IP66 standard.

III. NEW HELIUM REFRIGERATOR

The new liquid helium refrigerator (model-LR280 of Linde Kryotechnik AG) of specified refrigeration capacity 750W@4.2K or liquid production rate 180L/hr is installed commissioned and tested at IUAC. To operate the old and new helium refrigerator independently, separate room temperature helium gas piping between compressor, GMS and cold box was planned and installed. The plant had been tested upto 940W refrigeration capacity at 4.2K which is 25% higher than the specified refrigeration capacity. The refrigeration capacity might reach close to 1KW at little higher discharge pressure of new compressor. The liquefaction rate achieved was 206 L/hr. The old GMS had been relocated to accommodate the new compressor and GMS. Fig.3 and Fig.4 show the different components of the newly commissioned LR280 liquid helium refrigerator.

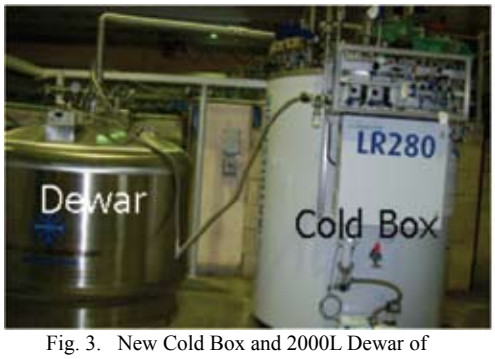

Fig. 3. New Cold Box and 2000L Dewar of New Helium Refrigerator

Fig. 4. Compressor and GMS of the New Helium Refrigerator

2.3.2 LINAC CRYOMODULES

During this academic year, for the first time, beam was accelerated through the LINAC-I and II cryomodules with sixteen resonators The LINAC-I and II cryomodules were cooled in series. During initial cool-down of both the cryomodules, the evaporated helium gas from LINAC-I cryomodule was passed through the LINAC-II cryomodule. The cooling scheme in LINAC II & III is different in comparison to the LINAC-I cryomodule. The two SS-support bars for resonators were cooled by the continuous thermo-siphonic flow using LN2 from LN2 vessel of the cryomodule. Fig.5 shows the cool-down profile of two SS-bars. This thermo-siphonic flow had brought down the equilibrium temperature of the support bars to 85K which is 125K for the LINAC-I cryomodule. LN2 precooling is avoided in the LINAC-II cryomodules prior to the helium cooling as the helium is fed to the bottom of the resonators.

Prior to the beam acceleration test, LINAC –II cryomodule with eight resonators was cooled to 4.2K for a separate off-line testing of the resonators. The average cooling rate for the resonators of LINAC-II cryomodule was more than 20K/hr (10K/hr for LINAC-I cryomodule) in the temperature range of 150K-80K. Fig.6 shows the typical cool-down curve of two resonators (R22 & R28) of LINAC-II cryomodules during off-line testing.

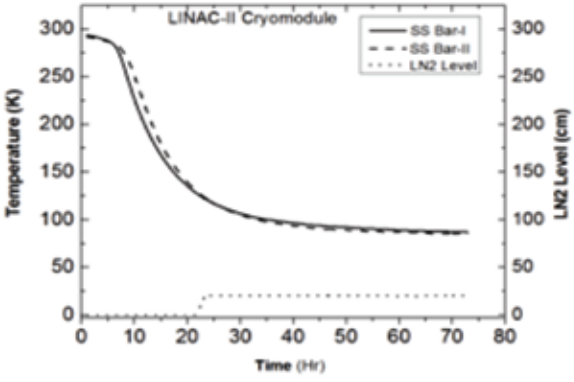

Fig. 5. The cool- down profile of resonator support bar

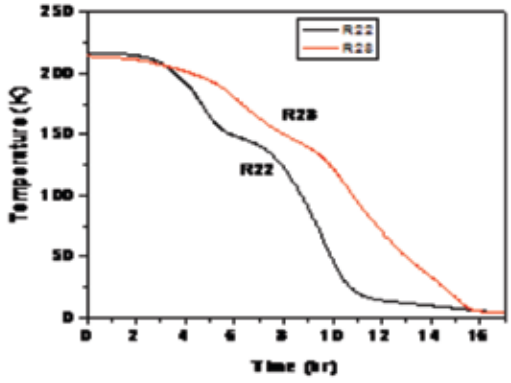

Fig. 6. The cool- down profile of R22 and R28 resonators of LINAC-II cryomodule

Though the cool-down rate of the resonators of the LINAC-II cryomodules was slower during series cooling with LINAC-I cryomodule, but no significant deterioration in accelerating field was observed in the resonators.

2.3.3 OTHER DEVELOPMENT PROJECTS

I. Superconducting (NbTi) Quadrupole Magnet Program for HYRA

Ten number of superconducting quadrupole coils were individually tested in the simple test cryostat (STC). The coils were charged upto 100A with maximum sweep rate 20A/min. Quenching had been observed in some of the coils during training at 4.2K. Eight coils had been mounted in the two iron yolks of the super-ferric magnet assembly as shown in Fig.5 and Fig.6. The inter-coil (NbTi-NbTi) resistive joints had been done on the copper bus bar with average overlap length of 175mm between two NbTi wires of two neighboring coils. There are six numbers of inter-coil NbTi-NbTi joints and four end leads for whole quadrupole doublets. The polarity of the coils in each singlet had been checked at room temp at 75mA current. The field profile has also been shown in the Fig. 7 and Fig. 8.

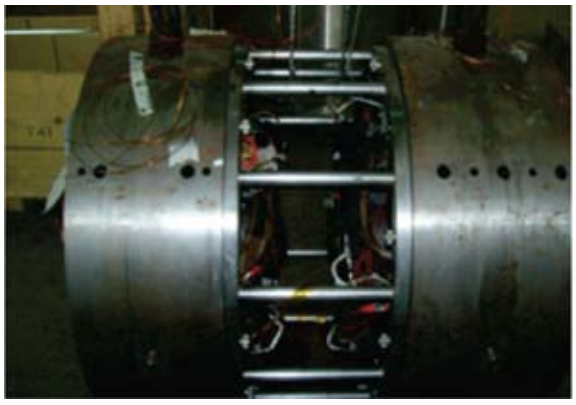

Fig. 5. Superconducting Quadrupole Magnet Assembly

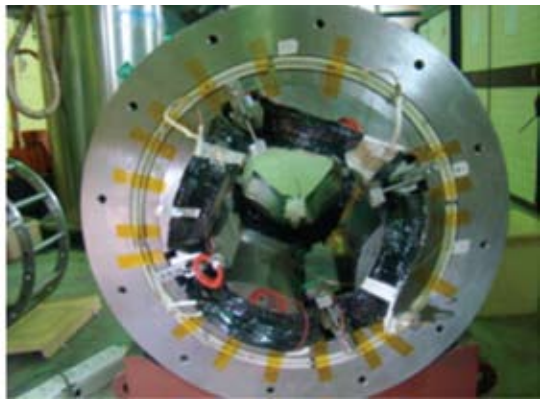

Fig. 6. The super-ferric magnet assembly

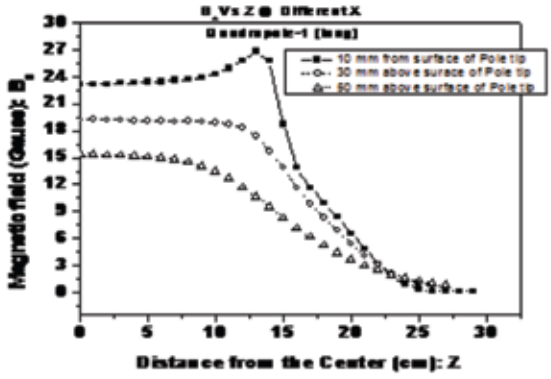

Fig. 7. The field profile (Bz) along the Z-axis

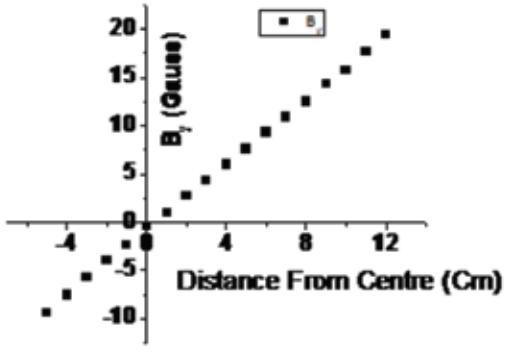

Fig. 8. The field profile (By) along the Y-axis.

II. Cryogen-Free Superconducting Magnet System (CFMS) –DST Project

A 6 T cryogen-free superconducting magnet system with room-temperature bore was developed in the last academic year. A few experimental measurements were carried out to evaluate the thermal conductance of the all thermal links between the cold head of the cryocooler and NbTi magnet. The dynamic thermal profile of the magnet during charging and discharging at different sweep rates had also been studied. The AC magnetization losses in the superconductor and other dynamic losses had been theoretically estimated during charging and discharging of the magnet and it has been correlated with the measured thermal profile.

A new project on the development of the variable temperature insert (VTI) to carry out experiments with temperature variation from 4.2K to 300K along with magnetic field variation from zero to 6T as an accessory of CFMS was proposed by us. The project is sanctioned by DST and it would be initiated shortly.

2.3.4 INSTRUMENTATION DEVELOPMENTS

I. Development of low cost Web-PLC

Field buses are traditionally used in the industrial automation for interconnecting devices like PLC, sensors and actuators. But, Ethernet has been emerged as a widely deployed preferred backplane solution in the recent past which is backward compatible and internet based. A compact low cost Web-PLC is designed

with indigenous analog/digital boards, an interconnecting server (Linux /Window OS) with Qt C++ as the language for GUI applications. Fig. 9 shows the picture of Web-PLC.

Fig. 9. The Picture of WEB-PLC

II. Upgradation of EBW Control System

The present control software of IUAC-EBW machine runs on a PC with Pentium-III processor with Windows 3.1 OS. Presently, most of the components of the control system have become obsolete after ten years of its installation at IUAC. Hence, for uninterrupted operation, a latest version of PC, PLC, CNC and control software with world wide support running on a more recent version of windows operating system has been ordered to M/S Techmeta, France and would be installed in the coming academic year.

Fig. 10. New cryogenic temperature monitor

III. New generation Cryogenic Temperature Monitors and Other Instruments for LINAC –II & III Cryomodules.

Advanced type of 12-channel cryogenic temperature monitors have been designed and developed with advanced features like Ethernet outputs in addition to 0-10 V outputs to VME, a touch interface with graphical display to read temperature in K (or °C or volt). Fig.11 shows the picture of new generation cryogenic temperature monitor installed in LINAC-II and III cryomodules. Similarly, some other instruments like FPGA based 16-channel RF power read-out linear controllers, RF-pulse conditioners and electronics for Stepper motor movement for eight stepper motors have also been designed and developed.